JOURNAL OF AIRCRAFT
Vol. 42, No. 4, July–August 2005

Spline-Based Airfoil Curvature Smoothing and Its Applications

W. Li* and S. Krist†
NASA Langley Research Center, Hampton, Virginia 23681

The performance of a transonic airfoil is directly related to the airfoil curvature profile and its smoothness. Whereas univariate data smoothing has been studied extensively, very little research has been conducted on curvature smoothing. Consequently, airfoil smoothing in design environments is largely based on heuristic methods, and there is an art to the generation of an unbiased smooth fit of the airfoil's curvature profile by the modification of its geometry. In this paper, the sum of squares of the third derivative jumps is used as a curvature smoothness measure for the development of a spline-based airfoil smoothing method, called constrained fitting for airfoil curvature smoothing (CFACS). CFACS can take out dramatic curvature oscillations with extremely small geometry changes and smooth an airfoil segment without creating curvature oscillations near the endpoints. Visually, CFACS generates an unbiased smooth fit of the curvature profile. Examples demonstrating the utility of CFACS show how the smoothing can be tailored to promote desirable characteristics in performance trade studies.

Nomenclature

A	=	matrix representing smoothness measure
c	=	chord length of airfoil
c_d	=	drag coefficient
c_l	=	lift coefficient
c_p	=	pressure coefficient
$f(t)$	=	function of t for $0 \le t \le 1$
$f^{(r)}(t)$	=	rth derivative of $f(t)$
$f_{\bar{\boldsymbol{y}}}(t)$	=	cubic spline interpolation of vector $\bar{\boldsymbol{y}}$
$f^{(3)}_{\bar{\boldsymbol{y}}}(t)$	=	third derivative of $f_{\bar{\boldsymbol{y}}}(t)$
M	=	freestream Mach number
n	=	number of data points
$\mathcal{S}(\bar{\boldsymbol{y}})$	=	smoothness measure of vector $\bar{\boldsymbol{y}}$
$\boldsymbol{t}$	=	column vector of $t_1, t_2, \ldots, t_n$
t_i	=	knot location of spline functions
w_i	=	positive weight in smoothness measure
$\boldsymbol{x}$	=	column vector of x coordinates of airfoil data
x_i, y_i	=	coordinates of point on the plane
$\boldsymbol{y}, \bar{\boldsymbol{y}}$	=	column vectors of y coordinates of airfoil data
β, δ	=	parameters for choosing leading-edge segment
ϵ	=	percentage error tolerance for smoothing
θ	=	control parameter ($0 \le \theta \le 1$) for smoothing
τ_i	=	positive weight for least-squares fitting
$\| \|$	=	2-norm of any vector

Introduction

FOR many applications, it is desirable to fit a set of ordered data points, $\{(t_1, y_1), (t_2, y_2), \ldots, (t_n, y_n)\}$ with $t_i < t_{i+1}$, by a nonoscillatory curve. This problem is referred to as data smoothing. Data smoothing uses some smoothness measure of the curve (such as the energy of the second derivative of the fitting curve) and seeks a balance between fitting the data and minimizing the smoothness measure. This idea goes back to Whittaker,[1] who proposed the use of the sum of squares of differences of y_i as the smoothness measure for equally spaced t_i. The widely used smoothing spline method, developed independently by Schoenberg[2] and Reinsch,[3] involves the following minimization problem:

$$\min_f \theta \sum_{i=1}^{n} \left[\frac{y_i - f(t_i)}{\tau_i} \right]^2 + (1-\theta) \int_{t_1}^{t_n} \left[f^{(r)}(t) \right]^2 \mathrm{d}t \qquad (1)$$

where θ is a smoothing parameter. Further details on Schoenberg's and Reinsch's works are provided by de Boor[4] (pp. 207–208). Wahba[5] and Green and Silverman[6] give complete treatises of the smoothing spline method from a statistical perspective. (Wahba also provides a comprehensive historical account; see the foreword in Ref. 5.) Most curve and surface smoothing formulations are variations of the smoothing spline method. Hoschek and Lasser[7] (pp. 553–556) summarize a number of formulations used in computer-aided geometric design.

In general, a smaller value of θ means a smoother fitting curve. However, it is difficult to choose a value of θ that will achieve the optimal balance between fitting and smoothing. Typically, the user inspects the fitting curves for various θ values, then chooses the fitting that is most desirable. To mitigate subjectivity in the smoothing process, statistical approaches, such as generalized cross validation, were proposed to estimate the optimal choice of θ (Refs. 5, 6, and 8). However, there is no guarantee that the resulting fitting spline will be what the user wants. As a compromise, Dierckx[9] developed a smoothing spline method that finds the smoothest fitting that satisfies a predetermined fitting error tolerance. The main idea in Dierckx's method is to choose a minimum set of knots such that least-squares fitting of the data by cubic splines with the set of knots is less than the specified error tolerance, then to find the cubic spline that satisfies the error tolerance while having the smallest sum of the squares of the third derivative jumps at the set of knots.

More recently, Lavery[10] studied a new spline smoothing method in which the 2-norm in Eq. (1) is replaced by the 1-norm. He proposed the following formulation for nonoscillatory data fitting:

$$\min_f \theta \sum_{i=1}^{n} |y_i - f(t_i)| + (1-\theta) \int_{t_1}^{t_n} \left| f^{(r)}(t) \right| \mathrm{d}t \qquad (2)$$

The rationale behind Eq. (2) is that the 1-norm fitting is less sensitive to outliers than the 2-norm fitting, making it less oscillatory.

Numerous local smoothing methods to improve the smoothness of a spline curve have also been proposed (Refs. 11–14 and pp. 563–568 in Ref. 7). These methods are mainly used for interactive fairing of spline curves in computer-aided geometric design.

For exact fitting of data, Akima's interpolation scheme[15,16] generates less oscillatory cubic piecewise polynomial curves than the cubic spline interpolation schemes. However, Akima's interpolation can generate fitting curves that are flatter than they should be.

Received 26 April 2004; revision received 29 June 2004; accepted for publication 15 July 2004.

*Senior Research Engineer, Multidisciplinary Optimization Branch; w.li@nasa.gov. Member AIAA.

†Aerospace Engineer, Configuration Aerodynamics Branch; steven.e.krist@nasa.gov. Member AIAA.

In Ref. 17, Akima discusses which geometric characteristics embedded in a data set should be preserved and proposes an improved interpolation method for generating "natural-looking" curves.

For airfoil designs under transonic flight conditions, where the pressure profile is closely related to the curvature profile of the airfoil, it is generally desirable to have airfoils with smooth curvature profiles. Hence, in smoothing the airfoil, it is important to preserve both the airfoil shape and main trends of the curvature profile while smoothing out undesirable curvature oscillations. However, most curvature smoothing methods pay no attention to the relationship between the curvature profiles of the original and fitting curves, as long as the fitting curves have smooth curvature profiles. See, for example, Ref. 18 and Sec. 23.2 in Ref. 14.

Wagner et al.[19] proposed the use of the spring spline method to smooth data with oscillatory curvature profiles. Their method solves a discrete version of the beam deflection equation [Eq. (26), Ref. 19] and finds a cubic spline fitting of the data points such that the discontinuity jump in the third derivative at a spline knot is a constant multiple of the fitting error at the same knot. However, the beam deflection equation is essentially a variational form of Eq. (1). As shown later, Eq. (1) can have undesirable smoothing characteristics, such as a tendency to retain low curvature characteristics even when the designer wants to smooth out a curvature dip of the airfoil.

Campbell[20] developed a local curvature smoothing procedure based on Akima's interpolation scheme for use in CDISC, an inverse design tool for aircraft wing design. Campbell's smoothing procedure can be described as follows: For each i, compute the value y_i^* of Akima's interpolation polynomial at x_i with the four nearest points to x_i, then replace y_i with $\lambda y_i + (1-\lambda)y_i^*$ with some weighting factor λ where $0 \le \lambda < 1$. Although Campbell's procedure is functional, a number of problems arise: The smoothed airfoil can exhibit substantial geometry deviations from the original airfoil, and when applied to an airfoil segment, the procedure can generate curvature oscillations at the endpoints of the segment.

In this paper, a new spline-based airfoil smoothing method, called constrained fitting for airfoil curvature smoothing (CFACS), is proposed. CFACS modifies the original airfoil as little as possible while smoothing the airfoil in such a way that the curvature profile of the modified airfoil becomes an "unbiased smooth fit" of the curvature profile of the original airfoil. The utility of CFACS is examined by smoothing curvature bumps on transonic airfoils for performance trade studies where the smoothing is tailored to promote desirable characteristics.

Airfoil Smoothing Problem

Because the upper and lower surfaces of transonic airfoils exhibit quite different curvature characteristics, it is preferable to smooth the two surfaces independently. Hence, the airfoil is decomposed into an upper surface, defined by a set of data points $\{(x_i^U, y_i^U) : 1 \le i \le n_U\}$, and a lower surface, defined by $\{(x_i^L, y_i^L) : 1 \le i \le n_L\}$, where $x_1^U < x_2^U < \cdots < x_n^U$, $x_1^L < x_2^L < \cdots < x_n^L$, and $x_1^U = x_1^L = y_1^U = y_1^L = 0$. Such a definition is typically extracted from a computational grid for the airfoil geometry, where data points are actual grid points on the airfoil surface. Consequently, data points tend to be clustered at both the leading edge (LE) and trailing edge (TE) of the airfoil.

For convenience, let $(\boldsymbol{x}, \boldsymbol{y})$ denote the data set $\{(x_i, y_i) : 1 \le i \le n\}$ that represents either surface of an airfoil, where $\boldsymbol{x}$ and $\boldsymbol{y}$ are column vectors whose ith components are x_i and y_i, respectively. The goal is to perturb the y coordinates of the data set $(\boldsymbol{x}, \boldsymbol{y})$ so that the modified data set represents an airfoil surface with a smooth curvature profile.

Note that, to manufacture an airfoil, a CAD definition of the airfoil surface is needed. Thus, it is natural to assume that the airfoil surface represented by $(\boldsymbol{x}, \boldsymbol{y})$ is actually defined by a parametric cubic spline interpolation of $(\boldsymbol{x}, \boldsymbol{y})$.

Formulations of the airfoil smoothing problem must then address three issues: 1) a parameterization for cubic spline representation of airfoil data, 2) a quantitative measure of visual smoothness of the curvature profile, and 3) an optimization procedure for the generation of a fitting with a smooth curvature profile. This section includes rationales for a knowledge-based spline parameterization, a definition of curvature smoothness, and formulation of the corresponding optimization problem for airfoil smoothing.

Parameterization for Preserving the LE Shape

One problem encountered by Campbell[20] during his development of a smoothing procedure for CDISC is that the use of smoothing to make an airfoil surface very smooth also tends to make the LE relatively flat. Because the LE shape has a pronounced impact on the flow characteristics, unwarranted smoothing of the LE is undesirable. Campbell mitigated this problem by using the parameterization $t_i = \sqrt{x_i}$, thereby applying smoothing to the transformed data set $\{(t_i, y_i) : 1 \le i \le n\}$ [denoted by $(\boldsymbol{t}, \boldsymbol{y})$]. This parameterization is based on "tribal knowledge" that the LE of a transonic airfoil is more or less like a parabolic curve $y^2 = \lambda x$ for some constant $\lambda > 0$. Now, with parameterization $t = \sqrt{x}$ and the LE approximation $y = \sqrt{\lambda} \cdot t$, the flatness of the smoothed data $(\boldsymbol{t}, \bar{\boldsymbol{y}})$ will not destroy the parabolic characteristics of the smoothed airfoil data $(\boldsymbol{x}, \bar{\boldsymbol{y}})$ near the LE.

Note that the parameterization $t = \sqrt{x}$ also solves the LE grid point clustering problem, making the spacing of points t_i relatively even except at the TE. However, if the airfoil LE rises faster than a parabolic curve, smoothing procedures using this parameterization tend to thin the airfoil near the LE. To protect against such a biased fit of the LE shape, the parameterization $t = x^\alpha$ is considered here. If $y^2 = \lambda x^{2\alpha}$ represents the LE shape and $t_i = x_i^\alpha$ for $1 \le i \le n$, then transformed airfoil data $(\boldsymbol{t}, \boldsymbol{y})$ has a flat LE segment and smoothing procedures have a minimal impact on the LE shape.

A simple estimate of α can be obtained by the computation of the interpolant $y^2 = \lambda x^{2\alpha}$ of the three points (x_1, y_1), (x_2, y_2), and (x_3, y_3). Based on the assumption of $x_1 = y_1 = 0$, the desired interpolant is completely determined by the following two conditions:

$$y_2^2 = \lambda x_2^{2\alpha}, \qquad y_3^2 = \lambda x_3^{2\alpha} \tag{3}$$

The elimination of λ in Eq. (3) yields an exponential equation, the solution of which is

$$\alpha = \frac{\log|y_3| - \log|y_2|}{\log|x_3| - \log|x_2|} \tag{4}$$

Because this definition of α is very sensitive to the three points near the LE and could be unreliable, a slight modification of the exponent is used, namely,

$$\bar{\alpha} = \frac{1}{3}\left(1 + \frac{\log|y_3| - \log|y_2|}{\log|x_3| - \log|x_2|}\right) \tag{5}$$

which is a weighted average of 0.5 and α.

By the use of the exponent defined in Eq. (5) for a nonlinear scaling of the x coordinates, $t_i = x_i^{\bar{\alpha}}$, a cubic spline function $g(t)$ is used to represent the transformed airfoil data $(\boldsymbol{t}, \boldsymbol{y})$. Many cubic splines $g(t)$ with knots $t_1 < t_2 < \cdots < t_n$ satisfy $g(t_i) = y_i$ for $1 \le i \le n$. Four boundary condition options for cubic spline interpolation [boundary conditions 1–4, pp. 43–45, Ref. 4] have been tested, and the "not-a-knot" condition gives the most natural curvature profile of the interpolating spline that represents an airfoil surface. Therefore, the cubic spline interpolation of $(\boldsymbol{t}, \boldsymbol{y})$ with the not-a-knot condition, denoted by $f_y(t)$, is used as the CAD definition of the transformed airfoil data $(\boldsymbol{t}, \boldsymbol{y})$. That is, $f_y(t)$ is the cubic spline function on the interval $[t_1, t_n]$ with knots $t_1 < t_2 < \cdots < t_n$ such that $f_y(t_i) = y_i$ for $1 \le i \le n$, and $f_y(t)$ is a cubic polynomial on the intervals $[t_1, t_3]$ and $[t_{n-2}, t_n]$, respectively. Note that t_2 and t_{n-1} are superfluous knots of $f_y(t)$ due to the not-a-knot condition.

Curvature Smoothness Measure of Airfoil Data

Because curvature fluctuations are mainly dominated by second derivative oscillations, an attempt might be made to use the energy of the third derivative as a quantitative measure of visual smoothness of the curvature profile. However, airfoils usually have extremely high curvatures near the LE. Because minimization of the energy of the third derivative reduces the magnitude of the LE curvature, its effects are undesirable. Moreover, sharp turns in the curvature

profile of an airfoil lower surface are often desirable features to be preserved during smoothing; minimization of the energy of the third derivative eliminates such sharp turns. For these reasons, the energy of the third derivative is not an appropriate smoothness measure for airfoils. As mentioned earlier, minimum energy splines or smoothing splines tend to reduce the magnitude of the curvature of fitting curves, generating biased fitting of the curvature profile even though they are unbiased smooth fittings of the airfoil shape.

The only choice remaining is to use a quantitative measure of the third derivative jumps of the cubic spline. In this paper, the sum of the squares of the third derivative jumps at the knots is used as the smoothness measure. The corresponding airfoil smoothing problem becomes a convex quadratic programming problem that can be easily solved.

With cubic spline representation of the data and the sum of the squares of the third derivative jumps at the knots as the smoothness measure of the cubic spline curve, the following smoothness measure of the data set $(\boldsymbol{t}, \boldsymbol{y})$ is introduced:

$$\mathcal{S}(\mathbf{y}) := \sum_{i=3}^{n-2} w_i \left[f_y^{(3)}\left(t_i^+\right) - f_y^{(3)}\left(t_i^-\right) \right]^2 \tag{6}$$

where $f_y^{(3)}(t_i^-)$ is the (constant) third derivative of f_y between t_{i-1} and t_i, and $f_y^{(3)}(t_i^+)$ is the third derivative of f_y between t_i and t_{i+1}. Expression (6), with $w_i = 1$, was first used as a smoothness measure by Dierckx.[9]

Weights in Smoothness Measure

Because $f_y^{(3)}(t_i^-)$ and $f_y^{(3)}(t_i^+)$ are linear functions of $\boldsymbol{y}$, there is an $(n-4) \times n$ matrix A such that

$$(A\mathbf{y})_{i-2} = \sqrt{w_i} \left[f_y^{(3)}\left(t_i^+\right) - f_y^{(3)}\left(t_i^-\right) \right] \tag{7}$$

for $3 \le i \le n-2$. Thus, $\mathcal{S}(\mathbf{y}) = \|A\mathbf{y}\|^2$. For airfoil data, $w_i = 1$ leads to an extremely ill-conditioned matrix A. Instead, values of w_i are chosen such that the maximum absolute value of elements in each row of A is exactly 1. Such a choice of weights in Eq. (6) is purely heuristic, and further study is necessary to understand its impact on curvature smoothness.

Basic Formulation of Airfoil Smoothing Problem

With the sum of the squares of the third derivative jumps at the knots as the curvature smoothness measure, the corresponding airfoil smoothing problem can be formulated as follows:

$$\min_{\bar{\mathbf{y}} \in \mathcal{F}} \theta \sum_{i=1}^{n} \left(\frac{y_i - \bar{y}_i}{\tau_i} \right)^2 + (1-\theta) \|A\bar{\mathbf{y}}\|^2 \tag{8}$$

where τ_i are positive numbers used to scale the fitting errors and $\mathcal{F}$ is the set of column vectors $\bar{\mathbf{y}}$ with n components $\bar{y}_1, \ldots, \bar{y}_n$ that satisfy certain constraints. These constraints include endpoint interpolation, airfoil thickness constraints, and curvature smoothness constraints.

Because the upper and lower surfaces are to be smoothed separately, the first and last points on both the upper and lower surfaces must be fixed. These constraints ensure that the smoothed surfaces will be connected at the LE and will not modify the thickness at the TE (whether blunt or sharp). Hence, any $\bar{\mathbf{y}} \in \mathcal{F}$ must satisfy the endpoint interpolation condition

$$\bar{y}_1 = y_1 \qquad \text{and} \qquad \bar{y}_n = y_n \tag{9}$$

Likewise, when smoothing a segment of the airfoil between chord locations x_{n_1} and x_{n_2} (with $1 \le n_1 < n_2 \le n$), the following constraints are imposed:

$$\bar{y}_i = y_i \qquad \text{for} \qquad 1 \le i \le n_1 \qquad \text{and} \qquad n_2 \le i \le n \tag{10}$$

An important constraint in airfoil design is on the thickness at specified chord locations. Consequently, it is usually necessary to restrict the smoothed airfoil, so that it satisfies the thickness constraints imposed on the original airfoil. The thickness constraints are defined as

$$\bar{y}_{i_k} = y_{i_k} \qquad \text{for} \qquad 1 \le k \le m \tag{11}$$

where m is the number of thickness constraints and $i_1, \ldots, i_m$ are indices such that x_{i_k} is the location where a thickness constraint is imposed.

Finally, it is desirable to avoid reductions in $\|A\bar{\mathbf{y}}\|^2$ through trades of the third derivative jumps at different knots because that allows the smoothed airfoil data to have more oscillatory curvature than $(\boldsymbol{x}, \boldsymbol{y})$ at some chord locations. The following pointwise smoothness constraints prevent such trades, ensuring that the smoothed airfoil data is smoother than $(\boldsymbol{x}, \boldsymbol{y})$ everywhere:

$$|(A\bar{\mathbf{y}})_i| \le |(A\mathbf{y})_i| \qquad \text{for} \qquad 1 \le i \le n-4 \tag{12}$$

Inequalities (12) guarantee that the jump in the third derivative of the spline $f_{\bar{y}}(t)$ at t_i is no more than the jump in the third derivative, $|f_y^{(3)}(t_i^+) - f_y^{(3)}(t_i^-)|$, of the interpolation spline $f_y(t)$ of the data $(\boldsymbol{t}, \boldsymbol{y})$ at t_i.

Choice of Smoothing Parameter

Let $\bar{\mathbf{y}}^*$ be an optimal solution of Eq. (8). If $\theta = 0$, then $A\bar{\mathbf{y}}^* = 0$, and $f_{\bar{y}^*}(t)$ is a cubic polynomial of t, a very smooth function. If $\theta = 1$, then $\bar{\mathbf{y}}^* = \mathbf{y}$, and no smoothing is performed. Unfortunately, it is difficult to relate the value of θ to the curvature smoothness of $(\boldsymbol{x}, \bar{\mathbf{y}}^*)$. Instead, Dierckx's approach[9] of specifying an error tolerance is employed. Here, the error tolerance is redefined slightly as a target value of $100\|\mathbf{y} - \bar{\mathbf{y}}^*\|/\sqrt{n}$ and represents the average percent error with respect to chord length. Because the fitting error $\|\mathbf{y} - \bar{\mathbf{y}}^*\|$ is a monotone function of θ, the required smoothing parameter for the given error tolerance ϵ is found in straightforward manner.

Knot Reduction for TE Smoothing

Typical computational grids for airfoils cluster grid points near the TE, making it difficult to smooth the curvature profile in this region. Fortunately, a fairly accurate spline approximation of an airfoil TE segment can be achieved without the use of all of the grid points near the TE as the spline knots.

The clustered grid points near the TE can be excluded from the knot sequence by replacement of the pointwise smoothness constraints near the TE with the following not-a-knot constraints:

$$|(A\bar{\mathbf{y}})_i| = 0 \qquad \text{for} \qquad n_0 \le i \le n-4 \tag{13}$$

where n_0 is selected so that the minimum value of the objective function $100\|\mathbf{y} - \bar{\mathbf{y}}\|/\sqrt{n}$ under constraints (10–13) is 0.05ϵ. That is, the error caused by the use of a cubic polynomial fitting near the TE is no more than 5% of the specified error tolerance. Constraints (13) are only used when $n_2 = n$.

LE Section Smoothing

The vertical tangent at the LE causes a major problem for airfoil smoothing methods in which only the y coordinates of the data points are to be modified. Let $x = x(t)$ and $y = y(t)$ be any parametric curve that represents an airfoil surface with the LE point $x(0) = 0$ and $y(0) = 0$. Consider the approach of modifying $y(t)$ to obtain a smoother function $\bar{y}(t)$. The curvature profile of the original curve, $\kappa(t)$, is given by

$$\kappa(t) = \frac{y''(t)x'(t) - x''(t)y'(t)}{([x'(t)]^2 + [y'(t)]^2)^{\frac{3}{2}}}$$

If the original curve has a vertical tangent at $t = 0$ and $y'(0)$ exists, then $x'(0)$ must be 0, yielding $|\kappa(0)| = |x''(0)|/\sqrt{|y'(0)|}$. Likewise, $|\bar{\kappa}(0)| = |x''(0)|/\sqrt{|\bar{y}'(0)|}$. That is, the LE curvature of the smoothed curve is completely determined by the first derivative of $\bar{y}(t)$ at $t = 0$, which is not controlled in the formulation of the problem. This lack of control near $t = 0$ leads to unpredictable values of $\bar{y}'(0)$.

Consequently, nonoscillatory behavior of the curvature profile near the LE cannot be guaranteed.

Alternatively, if a parametric curve $x = g(y)$ is used to represent an airfoil segment near the LE that encompasses both the upper and lower surfaces, then curvature oscillations are directly related to the behavior of the third derivative $g'''(y)$. In this form, the curvature over the LE section can be smoothed by modification of the x coordinates of the data points. To do so, it is necessary to define the range over which LE section smoothing is to be imposed. The basic idea is to find an LE section that can be parameterized as $x = g(y)$ and then identify a subsection on which the curve $x = g(y)$ is relatively flat for smoothing. To identify an LE section on a curve $x = g(y)$, find the y coordinates of the data points on the LE section that increase by at least a positive constant δ for two consecutive points. For smoothing, choose a relatively flat LE subsection on the curve $x = g(y)$, which can be accomplished when the slope is forced to be less than a given constant β. To define these two LE segments, let k_1^L, k_2^L, k_1^U, and k_2^U be the largest indices such that

$$\frac{x_{i+1}^L - x_i^L}{y_i^L - y_{i+1}^L} < \beta \qquad \text{for} \qquad 1 \le i < k_1^L$$

$$\frac{x_{i+1}^U - x_i^U}{y_{i+1}^U - y_i^U} < \beta \qquad \text{for} \qquad 1 \le i < k_1^U$$

$$y_i^L - y_{i+1}^L \ge \delta \qquad \text{for} \qquad k_1^L \le i < k_2^L$$

$$y_{i+1}^U - y_i^U \ge \delta \qquad \text{for} \qquad k_1^U \le i < k_2^U$$

Then the following data points define an LE section on a curve $x = g(y)$. Let $\{(\hat{x}_i, \hat{y}_i) : 1 \le i \le n\}$ be the relabeling of the airfoil data

$$\left(x_{k_2^L}^L, y_{k_2^L}^L\right), \ldots, \left(x_2^L, y_2^L\right), (0,0)$$

$$\left(x_2^U, y_2^U\right), \left(x_3^U, y_3^U\right), \ldots, \left(x_{k_2^U}^U, y_{k_2^U}^U\right) \tag{14}$$

Note that $n = k_2^U + k_2^L - 1$. The indices k_1^L and k_1^U are selected to ensure that $\{(\hat{x}_i, \hat{y}_i) : n_1 \le i \le n_2\}$ (with $n_1 = k_2^L - k_1^L + 1$ and $n_2 = n - k_2^U + k_1^U$) represents a relatively flat segment on the curve $x = g(y)$. In general, use $k_1^L < k_2^L - 4$ and $k_1^U < k_2^U - 4$ to ensure a smooth blending of the smoothed LE segment with the rest of the airfoil.

The LE section smoothing is formulated by redefinition of $t_i = \hat{y}_i$ and $y_i = \hat{x}_i$ for $1 \le i \le n$. The LE section is then smoothed from chord location $x_{k_1^L}^L$ on the lower surface (via the LE) to chord location $x_{k_1^U}^U$ on the upper surface by the solution of Eq. (8) with constraints (10) and (12).

Choice of Weighted Sum

Because of the sensitivity of the flowfield to the LE shape and the heuristic nature of the TE knot reduction strategy, it is desirable to limit geometry modifications at the LE and TE. This preference leads to the use of the following values for τ_i in Eq. (8):

$$\tau_i = \sqrt{[\tau_0 + |x_i(1 - x_i)|]/\tau_0} \qquad \text{for} \qquad 1 \le i \le n \tag{15}$$

where $\tau_0 > 0$ is a scaling factor. Note that if τ_0 is very large, then $\tau_i \approx 1$, and there is no scaling effect. If τ_0 is very small, then the solution $\bar{\boldsymbol{y}}^*$ of Eq. (8) fits the airfoil shape at the LE and TE more closely than at the midsection. The choice of τ_i is purely heuristic.

Airfoil Curvature Smoothing Method

All of the strategies given in the preceding subsections are combined to formulate the airfoil curvature smoothing algorithm CFACS.

CFACS

Let $\{(x_i^L, y_i^L) : 1 \le i \le n_L\}$ and $\{(x_i^U, y_i^U) : 1 \le i \le n_U\}$ denote the lower and upper surfaces of an airfoil, with $x_1^L < x_2^L < \cdots < x_n^L$, $x_1^U < x_2^U < \cdots < x_n^U$, and $x_1^L = x_1^U = y_1^L = y_1^U = 0$.

Upper or Lower Surface Smoothing

Step 1

Let $\{(x_i, y_i) : 1 \le i \le n\}$ be the data points on either the upper or lower surface. Compute $\bar{\alpha}$ given in Eq. (5). Use the parameterization $t_i = x_i^{\bar{\alpha}}$ for $1 \le i \le n$. Compute the matrix A in Eq. (7), where $f_{\boldsymbol{y}}(t)$ is the cubic spline interpolation of $(\boldsymbol{t}, \boldsymbol{y})$ by the use of the not-a-knot condition. Select n_1 and n_2 if a segment of the airfoil is to be smoothed; otherwise, set $n_1 = 1$ and $n_2 = n$. Choose $\tau_0 > 0$, for example 10^{-6}, and define τ_i as in Eq. (15).

Step 2

Pick an error tolerance ϵ and find θ such that the optimal solution $\bar{\boldsymbol{y}}^*$ of Eq. (8) with constraints given in Eqs. (10–13) satisfies $\|\boldsymbol{y} - \bar{\boldsymbol{y}}^*\| = \epsilon\sqrt{n}/100$.

Step 3

Inspect the curvature profile of the data set $(\boldsymbol{x}, \bar{\boldsymbol{y}}^*)$. Repeat step 2 by the increase or decrease of ϵ until a satisfactory smooth curvature profile of $(\boldsymbol{x}, \bar{\boldsymbol{y}}^*)$ is found.

LE Section Smoothing

Step 4

Choose $\delta = 0.001$ and $\beta = 0.02$. Let $\{(\hat{x}_i, \hat{y}_i) : 1 \le i \le n\}$ be the relabeling of the data points on the LE section as in Eq. (14). Define $t_i = \hat{y}_i$ and $y_i = \hat{x}_i$ for $1 \le i \le n$, $n_1 = k_2^L - k_1^L + 1$, and $n_2 = n - k_2^U + k_1^U$. Compute the matrix A in Eq. (7), where $f_{\boldsymbol{y}}(t)$ is the cubic spline interpolation of $(\boldsymbol{t}, \boldsymbol{y})$ by the use of the not-a-knot condition. Choose $\tau_i = 1$ for $1 \le i \le n$.

Step 5

Pick an error tolerance ϵ and find θ such that the optimal solution $\bar{\boldsymbol{y}}^*$ of Eq. (8) with constraints (10) and (12) satisfies $\|\boldsymbol{y} - \bar{\boldsymbol{y}}^*\| = \epsilon\sqrt{n}/100$.

Step 6

Inspect the curvature profile of the data set $(\boldsymbol{x}, \bar{\boldsymbol{y}}^*)$. Repeat step 5 by increasing or decreasing ϵ until a satisfactory smooth curvature profile of $(\boldsymbol{x}, \bar{\boldsymbol{y}}^*)$ is found.

Remarks: Whereas the upper and lower surfaces can be smoothed in any order, LE section smoothing should not be used until the curvature profile is smooth everywhere except near the LE. Otherwise, severe curvature oscillations at chord locations $x_{k_1^L}$ on the lower surface or $x_{k_1^U}$ on the upper surface are likely to induce oscillations in the LE curvature. Users may also want to modify the choices of δ and β to control the LE segment involved in the smoothing process.

One might also treat the airfoil as a parametric spline curve $x = x(t)$ and $y = y(t)$ and smooth both x and y coordinates simultaneously. The main difficulty in such an approach is the lack of interaction between the fitting of $x(t)$ and the fitting of $y(t)$. When error tolerances ϵ_x and ϵ_y are used to control the smoothing of the x and y coordinates, respectively, it is clear that an increase in both ϵ_x and ϵ_y will make the fitting curve smoother; however, the effect of an increase in ϵ_y while reducing ϵ_x is much more difficult to discern. The authors have experimented with a smoothing method similar to CFACS in which both x and y coordinates of the data are smoothed and found it very difficult to choose an appropriate ratio of ϵ_x/ϵ_y that leads to a desirable curvature smoothing effect.

There have also been attempts to smooth airfoils by modification of the shape in the normal directions. That is, to compute a normal vector (u_i, v_i) of the airfoil shape at (x_i, y_i) and use the parametric form $\bar{x}_i = x_i + \delta_i u_i$, $\bar{y}_i = y_i + \delta_i v_i$ for modification of (x_i, y_i) to smooth the airfoil. The objective is to find values of δ_i so that the modified airfoil data $\{(\bar{x}_i, \bar{y}_i) : 1 \le i \le n\}$ have a smooth curvature profile. The main advantage of this method is that it tries to modify

the x coordinates near the LE and the y coordinates over the relatively flat parts of the airfoil. The difficulty is that the normal vector $(\boldsymbol{u}_i, \boldsymbol{v}_i)$ is usually contaminated by noise in the airfoil data.

Numerical Results

The utility of CFACS as a curvature smoother has been examined by extensive tests on numerous supercritical airfoils generated with inverse design and optimization tools. This section documents selected numerical results demonstrating the behavior of CFACS, the reasons behind some of the choices made in the formulation of the method, and its use in airfoil performance trade studies.

In the examples to come, curvature profiles of the airfoil data are constructed from the following three-point approximation: Find the circle that fits the three points (x_{i-1}, y_{i-1}), (x_i, y_i), and (x_{i+1}, y_{i+1}), then use the reciprocal of the radius as the curvature at (x_i, y_i). Tests have shown that the three-point curvature profile accurately approximates the analytical curvature profile obtained from a cubic spline interpolation of the data. To reflect concavity in the airfoil shape, a negative sign is used to indicate that the shape is concave upward for the upper surface or concave downward for the lower surface. Under this convention, an airfoil as a boundary curve of a convex region has a positive curvature profile.

First consider an airfoil with 117 grid points on each surface ($n_L = n_U = 117$). The airfoil is smoothed by the application of CFACS on the lower and upper surfaces ($0 \le x/c \le 1$) with $\epsilon = 0.03$ and $\epsilon = 0.001$, respectively, followed by LE section smoothing with $\epsilon = 0.004$. Because airfoil curvature smoothing is a multiscale problem (large curvature near the LE and relatively small curvature elsewhere), several figures are required to distinguish variations in the curvature profile over different portions of the airfoil.

The effect of CFACS smoothing on the LE shape and curvature, with and without the use of LE section smoothing, is shown in Fig. 1. Without LE section smoothing (only the y coordinates of the data points modified), oscillations in the LE curvature remain. The use of LE section smoothing, where only the x coordinates of the grid points are modified, eliminates the oscillations. Note that the large curvature oscillations are caused by extremely small perturbations in the geometry at only a few grid points near the LE.

Over the midsection of the airfoil, the curvature is two orders of magnitude smaller than that at the LE (cf., Figs. 1 and 2). As shown in Fig. 2, CFACS gives an unbiased smooth fit of the midsection

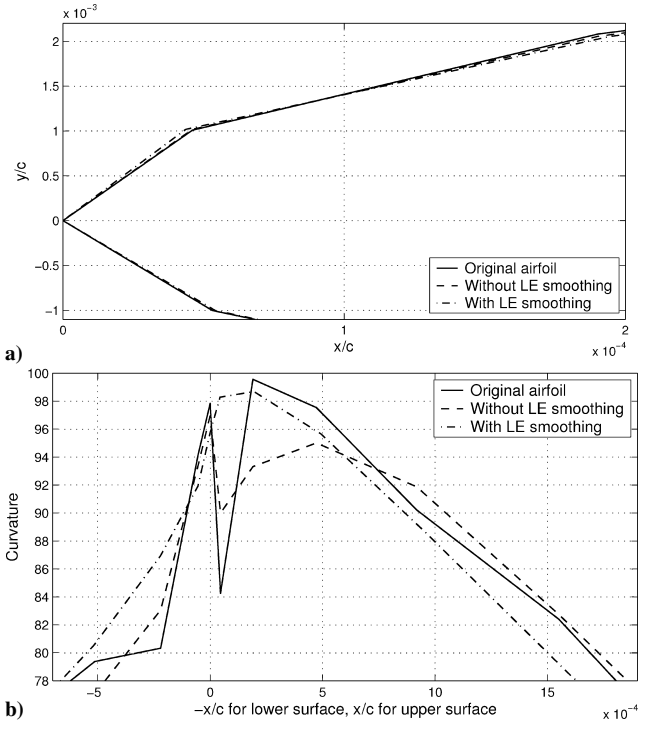

Fig. 1 LE a) shape and b) curvature for supercritical airfoil and its CFACS smoothing, without and with LE section smoothing.

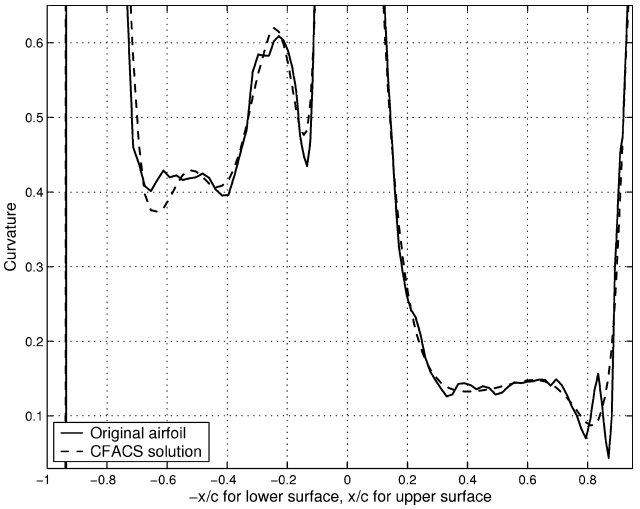

Fig. 2 Midchord curvature profiles for supercritical airfoil and its CFACS smoothing.

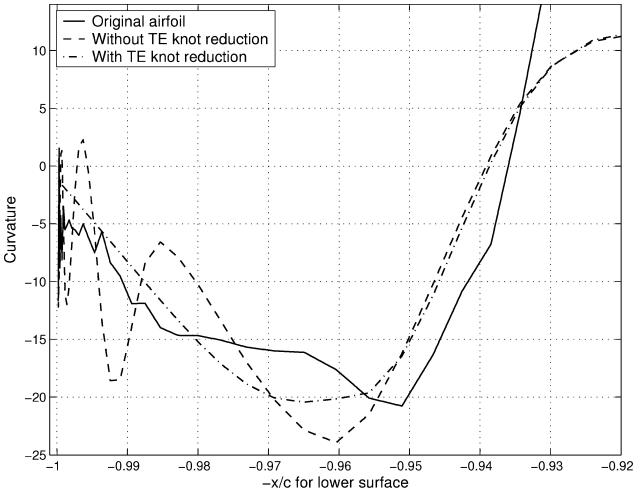

Fig. 3 Lower surface TE curvature profiles of supercritical airfoil and its CFACS smoothing, without and with knot reduction strategy.

curvature profile. Details of the lower surface TE curvature, shown in Fig. 3, indicate that the lower surface shape changes from concave upward to concave downward near $-x/c = -0.94$ and demonstrate the need for the knot reduction strategy. Because of the clustering of grid points near the TE, smoothing without constraints yields unnecessary curvature oscillations from $-x/c = -1$ to -0.96. Use of the knot reduction strategy, as detailed in Eq. (13), eliminates the extraneous oscillations while having an insignificant impact on the TE shape.

Because the flowfield is very sensitive to the LE shape, it is desirable to preserve the LE characteristics of the original airfoil when smoothing. To demonstrate the impact of parameterization on the LE shape, the entire upper surface of a supercritical airfoil is smoothed with $\epsilon = 0.03$ by the use of the two parameterizations discussed earlier, namely, $t = \sqrt{x}$ and $t = x^{\bar{\alpha}}$. The LE shape in Fig. 4 indicates that both parameterizations generate an LE shape that deviates from the original, but the $t_i = x_i^{\bar{\alpha}}$ parameterization yields a better LE fitting. Figure 4 also shows the effect of using equal weights τ_i in Eq. (8), rather than the weighted sum of Eq. (15). Clearly, the use of equal weights can lead to severe LE thinning.

The next example is provided to demonstrate differences between CFACS and the spline smoothing method. To ensure consistency in the parameterizations, the same knot sequence $t_i = x_i^{\bar{\alpha}}$, $1 \le i \le n$, is used for the spline smoothing method, which employs Eq. (1) with cubic splines and $r = 2$. The subroutine SMOOTH (details on p. 211 in Ref. 4) in the NETLIB library is used to generate the

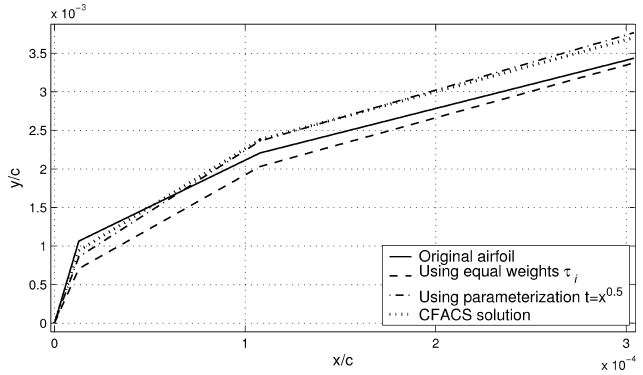

Fig. 4 Various strategies dealing with LE shape preservation.

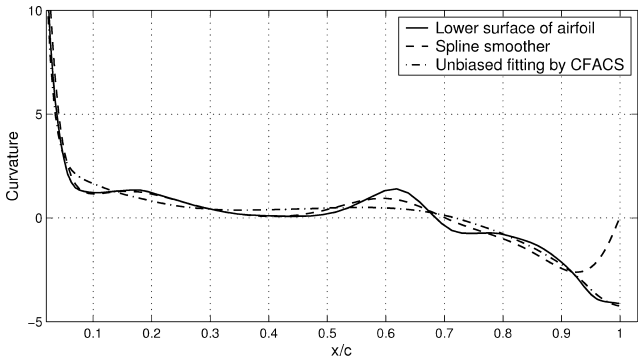

Fig. 5 Lower surface curvature profiles for supercritical airfoil, its spline smoothing, and CFACS smoothing.

smoothing spline. The interpolation of two endpoints, $f(t_1) = y_1$ and $f(t_n) = y_n$, is enforced by adjustment of the weights in SMOOTH to $\tau_1 = \tau_n = 10^{-15}$ and $\tau_i = 1$ for $1 < i < n$.

For illustration purposes, the entire lower surface (with $n_L = 101$) of a fairly smooth supercritical airfoil is smoothed by both SMOOTH and CFACS with $\epsilon = 0.09$. The results are shown in Fig. 5. Note that the biased curvature fit by SMOOTH near the TE is not due to the choice of θ; any other choice of θ with fitting error no less than 0.01 has a similar effect near the TE. As mentioned earlier, spline smoothing methods tend to minimize the curvature profile, which is undesirable for airfoil curvature smoothing.

With an understanding of how the curvature profile affects the flow physics, performance trade studies can be conducted by adjustment of the curvature smoothing to promote desirable characteristics. Three distinct airfoil designs are considered, all of which start from a Whitcomb 11%-thick integral supercritical airfoil (see Ref. 21) as the baseline, with $n_L = n_U = 101$. To preclude the enhancement of performance by airfoil thinning, the thickness is maintained at two spar locations ($x/c = 0.15$ and 0.60) and at the maximum thickness location.

The first example, a point design conducted with the CDISC inverse design method,[20] is primarily used to demonstrate the relationship between transonic flow characteristics and airfoil curvature. The transonic cruise design point is set at $M = 0.74$ with the lift coefficient specified as $c_l = 0.7$. Pressure coefficient distributions, upper surface curvature profiles, and drag rise curves for the baseline, the inverse design (designated as D1), and a CFACS smoothed design are shown in Fig. 6.

Design D1 is generated by the use of a typical procedure for the improvement of single-point performance; LE suction is largely preserved, and shock strength is reduced by a shift in the shock aft and the lowering of the roof top leading into the shock. The surface curvature profile for the design exhibits a classical shock bump centered at $x/c = 0.38$, which corresponds to the location of the top of the shock. To eliminate the shock bump, CFACS is used to smooth over the segment $0.02 \le x/c \le 1$ with $\epsilon = 0.01$. The smoothing results in a mild expansion before the shock that shifts the shock forward and increases its strength.

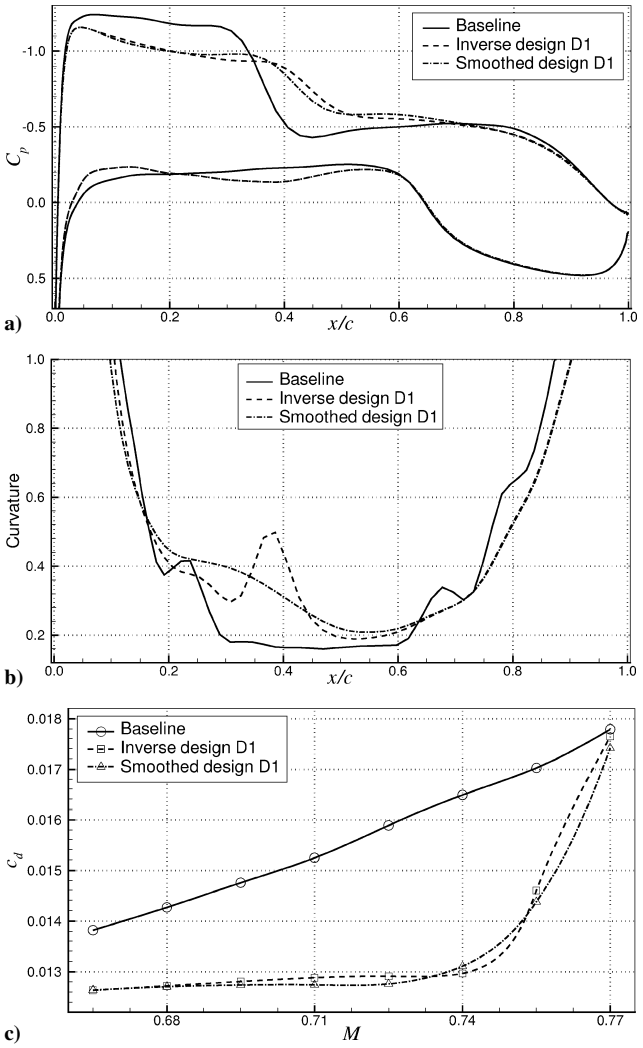

Fig. 6 Pressure coefficient distribution at a) $M = 0.74$ and $c_l = 0.7$, b) upper surface curvature, and c) drag rise curves at $c_l = 0.7$, for baseline and inverse design D1, unsmoothed and smoothed.

Drag rise curves for the three airfoils indicate that design D1 provides substantial performance improvements over the baseline at all Mach numbers below 0.77. Despite the magnitude of the shock bump, smoothing has a relatively mild effect on the performance characteristics of the airfoil. Nonetheless, smoothing enhances the performance at all of the off-design points. The expense for this improvement is a degradation in performance at the design point.

This example illustrates the danger in the "start with a dog" principle in design method promotion, wherein any design procedure can be shown to improve performance dramatically provided that the baseline is sufficiently inappropriate for the application at hand. (Here the baseline airfoil represents 1966 technology and was designed at $M = 0.80$ and $c_l = 0.65$.) In this case, where performance differences between the design and baseline are much larger than those between the unsmoothed and smoothed designs, one might well question the significance of smoothing. However, a recent estimate for a modern transonic transport indicates that a one-count reduction in drag ($c_d = 0.0001$) is worth $500,000 per year in fuel costs. Consequently, the mild tailoring of the drag rise curve shown here is significant at the level of detail to which wing designers work in refining a design.

The second design problem is representative of the conditions typically employed in demonstrating optimizers for multipoint airfoil design. Design points are specified at $M = 0.68$, 0.71, 0.74, and 0.77, with $c_l = 0.7$. The design is generated by the use of a recently developed airfoil shape optimization method for robust performance.[22]

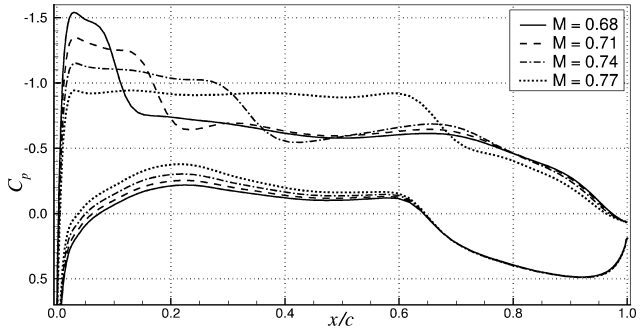

Fig. 7 Pressure coefficient distributions for optimized design D2 at $c_l = 0.7$.

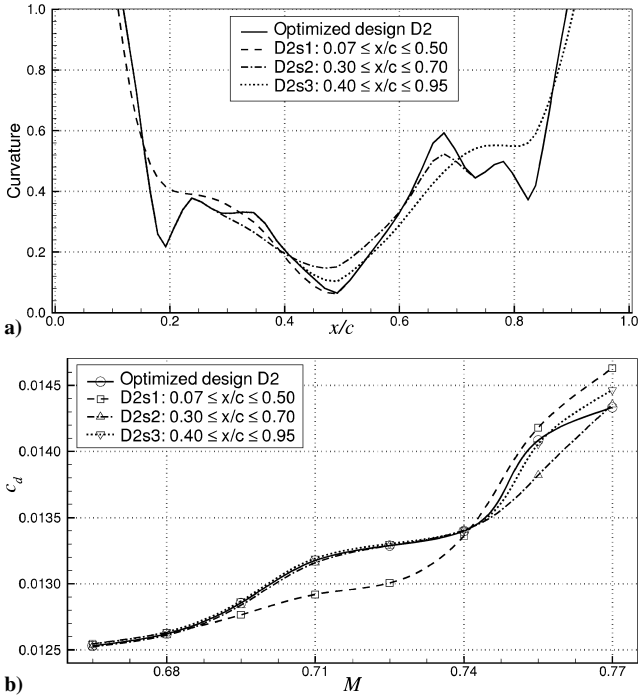

Fig. 8 Optimized airfoil D2 with smoothing over three different segments: a) upper surface curvature and b) drag rise curves.

Pressure coefficient distributions at the four design points and the upper surface curvature profile for the design (designated as D2) are shown in Figs. 7 and 8, respectively. Comparison of the shock locations with the curvature profile indicates that the pronounced bump at $x/c = 0.68$ is associated with the shock at $M = 0.77$. However, the bump at $x/c = 0.23$ begins well aft of the shock at $M = 0.71$ and forward of the shock at $M = 0.74$. This type of result makes it difficult to interpret why an optimizer does what it does.

The sharp variations in curvature for this design make it an excellent test bed for the exploration of smoothing strategies. To understand the effects of curvature oscillations on the performance of D2, CFACS is applied with an error tolerance of $\epsilon = 0.03$ over three separate segments on the upper surface: $0.07 \le x/c \le 0.5$ to smooth the first curvature trough (designated as D2s1), $0.3 \le x/c \le 0.7$ to smooth the midchord curvature trough (D2s2), and $0.4 \le x/c \le 0.95$ to smooth the back peak and trough (D2s3). The resulting curvature profiles are also shown in Fig. 8. Note that the smoothed segments blend smoothly with the fixed segments in each case.

Comparison of the drag rise curves for the four airfoils (also shown in Fig. 8) indicate that smoothing out the first curvature trough (D2s1) provides a significant performance enhancement at the mid-Mach numbers at the expense of higher drag at $M = 0.77$. Hence, this feature was generated to assist in the reduction of the drag at higher Mach numbers, even though it occurs well ahead of the shocks at those conditions. Smoothing out the midchord trough (D2s2) has little effect everywhere except at the intermediate Mach number $M = 0.755$. This type of result, where off-design performance is significantly improved with no degradation in performance elsewhere, illustrates a major motivation for smoothing. Smoothing the back end (D2s3) has little effect except at $M = 0.77$, for which the drag increases. One can tailor the back end smoothing to keep the drag at $M = 0.77$ from increasing, for example, start the segment smoothing from 0.5 rather than 0.4; however, there is usually a strong tradeoff between the performance at $M = 0.755$ and 0.77.

In the preceding examples, thickness constraints are not used in smoothing because constrained smoothing over relatively small segments usually restrains CFACS from making appreciable curvature changes. Over larger segments, smoothing with thickness constraints has a more benign effect. This effect is demonstrated when both unconstrained (D2s4) and constrained (D2s5) smoothing are conducted over the upper surface segment $0.05 \le x/c \le 0.90$ with $\epsilon = 0.02$; results are shown in Fig. 9. The constrained smoothing preserves the thickness at two spar locations ($x/c = 0.15$ and 0.6) and the maximum thickness location. The curvature profiles indicate that the constrained smoothing deviates somewhat less from the baseline curvature profile than unconstrained smoothing. The constrained smoothing has a positive effect on drag at higher Mach numbers centered around $M = 0.74$, whereas it has a smaller, negative effect at lower Mach numbers centered around $M = 0.695$. Of course, the primary reason for employment of the constraints is to preclude their violation. In this case, the unconstrained smoothing reduces the maximum thickness by 0.2% but still satisfies the two spar constraints.

Parametric studies on the length of smoothed segments and the value of the error tolerance on both the upper and lower surfaces of D2 were conducted for constrained smoothing. The lower surface proves to be quite insensitive to smoothing. Even the use of a large error tolerance ($\epsilon = 0.04$) over the full chord has a negligible effect on performance, though that effect is negative everywhere. Smoothing the upper surface near the LE, for example, over $0.003 \le x/c \le 0.07$, has a negative effect on low Mach performance while providing a more modest positive effect at high Mach numbers. Smoothing a large chord segment all of the way to the TE, for example, over $0.05 \le x/c \le 1$ rather than over $0.05 \le x/c \le 0.9$, has a small negative effect on performance everywhere. However, with a midchord segment being smoothed, additional smoothing over the back end of the airfoil has a positive effect. This result is demonstrated by

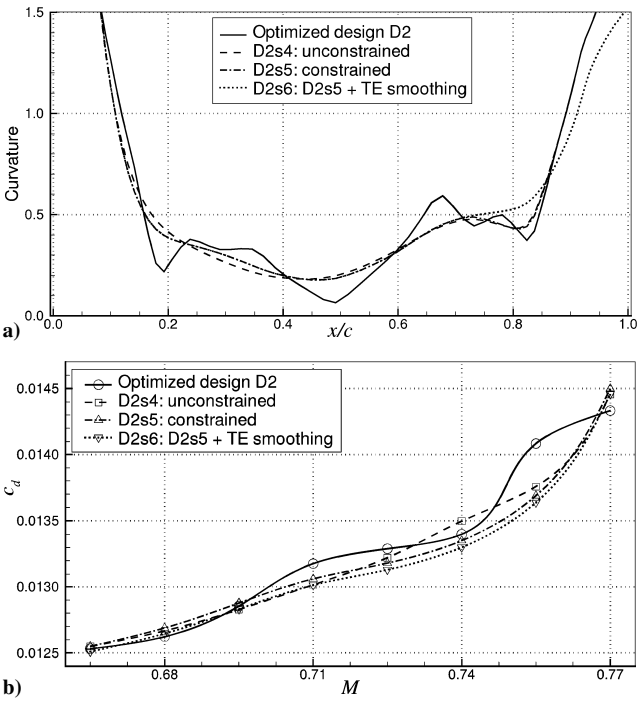

Fig. 9 Comparisons for optimized airfoil D2 with unconstrained and constrained smoothing: a) upper surface curvature and b) drag rise.

airfoil D2s6, where the back end of airfoil D2s5 is smoothed from $0.7 \le x/c \le 1$ with $\epsilon = 0.05$. The results in Fig. 9 indicate that the additional smoothing is worth a one-half-count reduction in drag everywhere except at $M = 0.77$, for which the drag reduction is more modest. Note that smoothing all of the way to the TE with a large error tolerance can dramatically thin the airfoil near the TE; however, this is not an issue in this case.

Based on these and other results, the preferred strategy developed for CFACS is to use a fairly strong segment smoothing or a sequence of segment smoothing on the upper surface, followed by a mild smoothing on the entire upper surface ($\epsilon = 0.001$), a somewhat stronger lower surface smoothing ($\epsilon = 0.01$), and a mild LE section smoothing ($\epsilon = 0.001$). Users should then tailor the upper surface segment smoothing to promote desirable characteristics.

Three examples of tailored smoothing are shown in Fig. 10. Airfoil D2s7 is constructed by smoothing over the segment $0.04 \le x/c \le 0.5$ with $\epsilon = 0.02$, then $0.04 \le x/c \le 0.9$ with $\epsilon = 0.01$, then $0.7 \le x/c \le 1.0$ with $\epsilon = 0.03$, followed by the full chord and LE section smoothing prescribed earlier. The intent here is to smooth the forward and midcurvature troughs to improve the performance at the mid-Mach numbers and $M = 0.755$, respectively, while the elevated curvature around $x/c = 0.7$ is preserved to preserve the performance at $M = 0.77$. The drag rise curve indicates that performance is better than the baseline at all mid-Mach numbers, whereas it is only slightly worse at the lowest and highest Mach numbers. Airfoils D2s8 and D2s9 are constructed by smoothing with $\epsilon = 0.03$ over the segments $0.04 \le x/c \le 0.87$ and $0.02 \le x/c \le 0.9$, respectively, followed by smoothing from $0.7 \le x/c \le 1$, followed by the use of the full chord and LE section smoothing prescribed earlier. The drag rise curves indicate that D2s8 trades performance at $M = 0.77$ for improvements at $M = 0.755$, whereas D2s9 trades performance at both ends of the Mach range for additional improvements at the mid-Mach numbers. Note that the authors were not able to smooth D2 in a manner that improves performance at both ends of the design range ($M = 0.68$ and 0.77) without significant degradations in the mid-Mach performance.

In the last example for this case, the advantage of CFACS smoothing over the local smoothing method implemented in CDISC is demonstrated. A comparison for unconstrained smoothing is not particularly meaningful because the Akima interpolation method employed in CDISC reduces the airfoil thickness to a much greater extent than similar smoothing from CFACS. To implement a constrained smoothing within CDISC, subsequent to the smoothing, a variable scaling of the airfoil is employed to match the thickness constraints. To keep the comparison as simple as possible, CDISC smoothing is applied over the same upper surface segment smoothed in D2s5 ($0.04 \le x/c \le 0.9$), with 100 iterations; results are shown in Fig. 11.

The curvature profile for the airfoil smoothed by CDISC, designated as D2s10, is quite similar to that from CFACS, except near the end of the segment where the last trough is smoothed out a bit more. However, the shape of the D2s10 airfoil deviates from the baseline shape quite a bit more than D2s5. In fact, due to the use of scaling to meet the thickness constraints, the shape of D2s10 changes well in front of $x/c = 0.04$, leading to a blunter LE. The impact of these differences on the drag is seen primarily from $M = 0.71$ to 0.77, for which the performance of D2s10 is significantly worse than D2s5. Attempts to correct this deficiency by smoothing over a number of segments proved unsuccessful because the CDISC smoothing tends to generate undesirable curvature bumps at the end of the smoothed segments.

The third design problem is representative of the type of conditions typically used in industrial multipoint design efforts. Three design points are used to represent the start, middle, and end cruise conditions ($c_l = 0.76$, 0.70, and 0.64, respectively, at the cruise speed $M = 0.76$), with a lower speed design condition ($M = 0.70$, $c_l = 0.70$) used to limit degradation in the climbout performance. The robust optimization method employed in design D2 is used here as well.

Results for the optimized design (designated as D3) and a CFACS smoothing are shown in Fig. 12. Here, CFACS is applied to smooth two upper surface segments, first over $0.02 \le x/c \le 0.8$; then over $0.02 \le x/c \le 0.99$ (both with $\epsilon = 0.03$), followed by the full chord and LE segment smoothing prescribed earlier. Note that an additional smoothing over segments near the TE of the airfoil is not used here because it causes the airfoil near the TE to become impractically thin.

Drag rise curves for design D3 exhibit a drag rise bucket at all three cruise conditions, wherein the drag does not increase monotonically over the Mach range ($0.66 \le M \le 0.76$). The bucket, which becomes more pronounced with increasing lift coefficient, is undesirable in that it is associated with a performance penalty in the climbout to cruise, and climbout performance is a factor in sizing

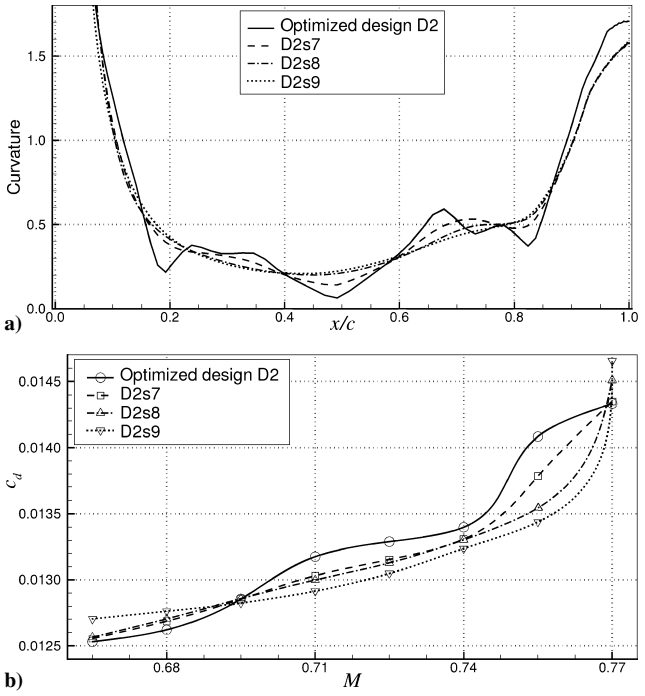

Fig. 10 Comparisons for smoothing optimized airfoil D2 with three tailored smoothing strategies: a) upper surface curvature and b) drag rise.

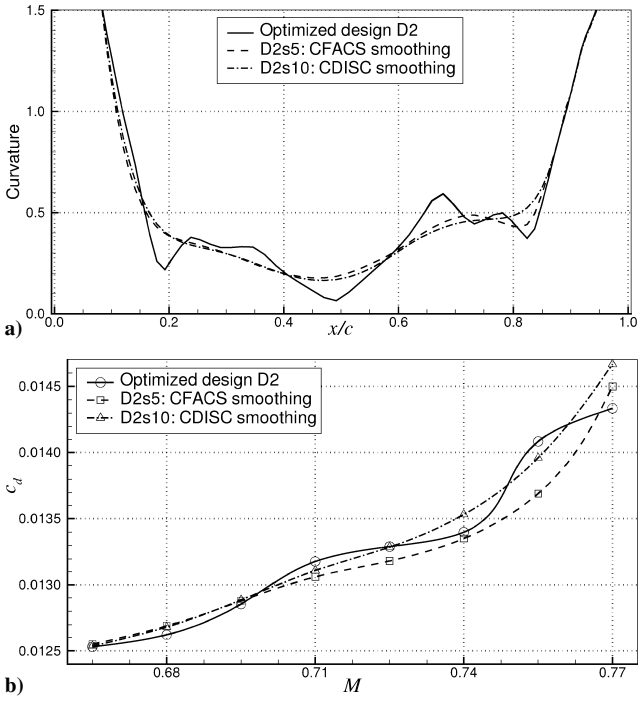

Fig. 11 Comparisons for optimized airfoil D2 with CFACS and CDISC constrained smoothing: a) upper surface curvature and b) drag rise.

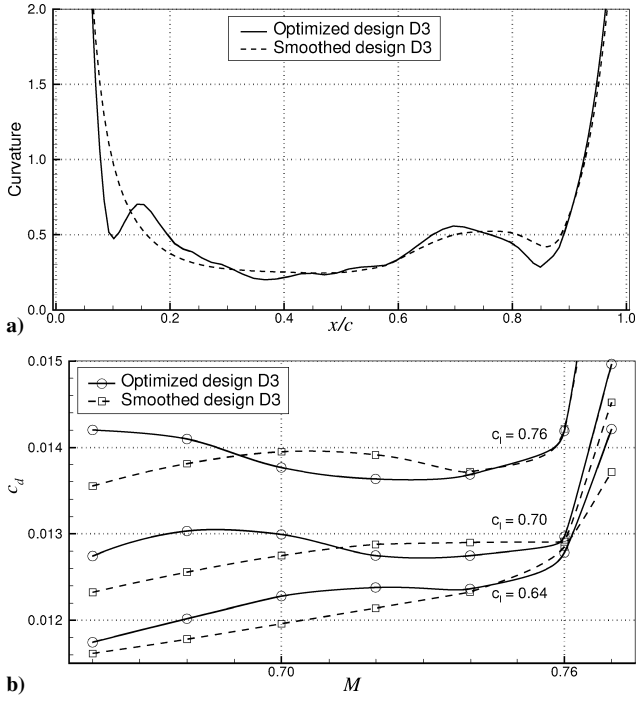

Fig. 12 Optimized airfoil D3, unsmoothed and smoothed: a) upper surface curvature and b) drag rise comparison at $c_l = 0.64$, 0.70, and 0.76.

the engines. The smoothed airfoil eliminates the buckets at the lower lift coefficients and softens the bucket at $c_l = 0.76$, with substantial reductions in drag at the lower Mach numbers.

The expense for changing the character of the drag rise curves is a degradation in performance at mid-Mach numbers for the two high-lift coefficient conditions and at the design point for $M = 0.76$ and $c_l = 0.64$. In fact, substantial effort was required to tailor the smoothing to preserve as much of the performance at $M = 0.76$, $c_l = 0.64$ as possible. It was found that any significant smoothing of the aft curvature bump leads to the formation of a double shock at this condition that quickly leads to significant increases in the drag. Whereas the smoothed airfoil significantly improves the overall characteristics of the design, it does not fix it; specifically, the drag rise bucket for $c_l = 0.76$ has not been eliminated. In practice, the designer would need to go back and reoptimize the configuration with a stronger preference on optimizing the performance at both the end cruise and the low Mach design conditions.

The preceding examples demonstrate that with knowledge of how the airfoil curvature profile affects the flow characteristics, CFACS can be used to tailor the curvature to provide modest alterations in the airfoil performance characteristics and to eliminate unnecessary curvature oscillations. Moreover, the results suggest that variance in the performance of a smoothed airfoil will be less than that of an unsmoothed airfoil. However, the tailoring can require a rather complex specification of multiple smoothing segments and error tolerances. It is an exploratory process, where analyses of the smoothed airfoils are used to understand the effects of curvature bumps on airfoil performance.

In general, one can get very satisfactory smoothing results by running CFACS a few times with fitting error tolerance ϵ ranging from 0.001 to 0.05 for upper or lower surface smoothing, though care must be taken with smoothing the upper surface LE. The LE section smoothing can usually be achieved by the use of an extremely small error tolerance, with little if any effect on the flow characteristics of the underlying airfoil. Except at the LE, the solution of CFACS always has a smoother curvature profile than the original airfoil everywhere. When used to smooth an airfoil segment, CFACS always blends the fixed segments and the smoothed segment without creating any curvature oscillations at the endpoints of the smoothed segment. This property is essential when the smoothing is tailored in trade studies.

Conclusions

In this paper, the sum of squares of the third derivative jumps of the cubic spline interpolation of airfoil data is used as a curvature smoothness measure of the data. A formulation for minimization of the smoothness measure within a specified fitting error tolerance is developed. This formulation is incorporated in a tool called CFACS that is used for smoothing an airfoil segment while preserving the thickness at specified chord locations.

CFACS is a combination of rigorous mathematical modeling and knowledge-based heuristics. Rigorous mathematical formulation assures users that CFACS will take out undesirable curvature oscillations with minimum modification of the airfoil geometry. Knowledge-based heuristics bridge the gap between theory and best practices by designers.

CFACS has been extensively tested on a number of supercritical airfoils generated from inverse design and optimization tools. All of the smoothing results show that CFACS is able to generate unbiased smooth fitting of the curvature profiles, trading small geometry modifications for dramatic improvements in curvature smoothness by eliminating curvature oscillations and bumps. The demonstrated capabilities of CFACS indicate that it is a powerful tool for the clean-up of airfoil curvature oscillations and to smooth out curvature bumps for transonic airfoil performance trade studies.

For aircraft wing design, the shape of the wing can be defined by a finite set of airfoil sections connected in the spanwise direction by a smooth surface (such as a bivariate B-spline or NURBS). Because the airfoil sections from computational designs typically embody undesirable curvature oscillations, a tool based on CFACS would provide a powerful means for the clean-up of the design wherein the change in shape is minimized. Moreover, a wing curvature smoothing problem could be formulated by the use of the sum of squares of the third derivative jumps as a curvature smoothness measure for a bicubic B-spline representation of the wing. However, due to relatively small curvature changes in the spanwise direction, it might be more meaningful to use the magnitude of the first or second directional derivative in the spanwise direction, along with the curvature smoothness measure for the airfoil sections.

Acknowledgments

The authors would like to thank Richard Campbell for helping us understand the smoothing procedure in CDISC.

References

[1]Whittaker, E., "On a New Method of Graduation," *Proceedings of the Edinburgh Mathematical Society*, Vol. 41, 1923, pp. 63–75.

[2]Schoenberg, I., "Spline Functions and the Problem of Graduation," *Proceedings of the National Academy of Sciences*, Vol. 52, 1964, pp. 947–950.

[3]Reinsch, C., "Smoothing by Spline Functions II," *Numerische Mathematik*, Vol. 16, 1971, pp. 451–454.

[4]de Boor, C., *A Practical Guide to Splines (Revised Edition)*, Springer, New York, 2001, pp. 207, 208, 211.

[5]Wahba, G., *Spline Models for Observational Data*, Society for Industrial and Applied Mathematics, Philadelphia, 1990.

[6]Green, P., and Silverman, B., *Nonparametric Regression and Generalized Linear Models—A Roughness Penalty Approach*, Chapman and Hall, New York, 1994.

[7]Hoschek, J., and Lasser, D., *Fundamentals of Computer Aided Geometric Design*, A. K. Peters, Wellesley, MA, 1993, pp. 553–556, 563–568.

[8]Keren, D., and Werman, M., "A Full Bayesian Approach to Curve and Surface Reconstruction," *Journal of Mathematical Imaging and Vision*, Vol. 11, 1999, pp. 27–43.

[9]Dierckx, P., *Curve and Surface Fitting with Splines*, Oxford Univ. Press, Oxford, England, U.K., 1993.

[10]Lavery, J., "Shape-Preserving, Multiscale Fitting of Univariate Data by Cubic L_1 Smoothing Splines," *Computer Aided Geometric Design*, Vol. 17, 2000, pp. 715–727.

[11]Kjellander, J., "Smoothing of Cubic Parametric Splines," *Computer-Aided Design*, Vol. 15, 1983, pp. 175–179.

[12]Farin, G., Gein, G., Sapidis, N., and Worsey, A., "Fairing Cubic B-Spline Curves," *Computer-Aided Geometric Design*, Vol. 4, 1987, pp. 91–104.

[13]Poliakoff, J., "An Improved Algorithm for Automatic Fairing of Non-Uniform Parametric Cubic Splines, *Computer-Aided Design*, Vol. 28, 1996, pp. 59–66.

[14]Farin, G., *Curves and Surfaces for CAGD: A Practical Guide*, 5th ed., Morgan Kaufmann, San Mateo, CA, 2001, Sec. 23.2.

[15]Akima, H., "A New Method of Interpolation and Smooth Curve Fitting Based on Local Procedures," *Journal of the ACM*, Vol. 17, 1970, pp. 589–602.

[16]Akima, H., "Algorithm 433: Interpolation and Smooth Curve Fitting Based on Local Procedures [E2]," *Communications of the ACM*, Vol. 15, 1972, pp. 914–918.

[17]Akima, H., "A Method of Univariate Interpolation That Has the Accuracy of a Third-degree Polynomial," *ACM Transactions on Mathematical Software*, Vol. 17, 1991, pp. 341–367.

[18]Higashi, M., Tsutamori, H., and Hosaka, M., "Generation of Smooth Surfaces by Controlling Curvature Variation," *Eurographics*, Vol. 15, 1996, pp. 187–196.

[19]Wagner, P., Luo, X., and Stelson, K., "Smoothing Curvature and Torsion with Spring Splines," *Computer-Aided Design*, Vol. 27, 1995, pp. 615–626.

[20]Campbell, R., "Efficient Viscous Design of Realistic Aircraft Configurations," AIAA Paper 98-2539, June 1998.

[21]Harris, C., "NASA Supercritical Airfoils—A Matrix of Family-Related Airfoils," NASA TP-1990-2969, March 1990.

[22]Li, W., Krist, S., and Campbell, R., "Transonic Airfoil Shape Optimization in Preliminary Design Environment," AIAA Paper 2004-4629, Aug. 2004.